Ridge-waveguide sidewall-grating distributed feedback structures fabricated by x-ray lithography

Vincent V. Wong, Woo-Young Choi, J. M. Carter, C. G. Fonstad, and Henry I. Smith
Department of Electrical Engineering and Computer Science, Massachusetts Institute of Technology, Cambridge, Massachusetts 02139

Y. Chung and N. Dagli
Department of Electrical Engineering, University of California, Santa Barbara, Santa Barbara, California 93106

A novel distributed feedback structure has been developed in which the grating is patterned onto the sidewalls of a ridge waveguide. Such a laser structure results in simplified processing in that the grating fabrication is independent of both the materials growth and the guide formation. The ridge waveguide is first formed by wet-chemical etching. Then, a poly(methylmethacrylate) grating ($\Lambda=230$ nm) is patterned onto this ridge waveguide using x-ray lithography. A Ti/Al etch mask is lifted-off to serve as a mask for subsequent reactive-ion etching. Gratings with long-range spatial-phase coherence and negligible distortion, characteristics which are necessary for accurate control of the wavelength and bandwidth, are obtained using a holographically generated x-ray mask.

I. INTRODUCTION

Distributed feedback (DFB) structures, such as lasers and channel-dropping filters (CDFs)[1] are essential components in long-haul high-data-rate optical communication systems. DFB lasers operate in a single-longitudinal mode and are easily integrable with electronic drive circuitry and various passive optical components. CDFs, owing to their narrow bandwidth (~0.1 nm), are ideal for wavelength-division-multiplexing systems.[1] Both of these devices rely on either uniform or phase-shifted gratings, whose lengths range from ~0.2 to several millimeters.

Typically, in the fabrication of a DFB laser the formation of the grating interrupts the epitaxial growth of the layer structure, thereby requiring an overgrowth step.[2–4] Such an overgrowth results in increased process complexity. Recently, Miller et al.[5] proposed a laser structure in which lateral gratings, patterned with e-beam lithography (EBL), are reactive-ion etched in the top confining layer of the laser on either side of the contact stripe. The gratings serve to provide both optical feedback and lateral optical confinement, which are dependent on grating depth. This process, while requiring only one epitaxial growth step, is complicated by the fact that extremely deep (~0.7–1.0 μm) gratings are required. Korn et al.[6] proposed a laser structure in which the grating is patterned on top of the ridge by EBL followed by reactive-ion etching (RIE).

We are developing a novel DFB structure in which the gratings are etched into the sidewalls of the ridge waveguide. The gratings are patterned by x-ray lithography (XRL) with a holographically generated x-ray mask (Λ =230 nm). XRL offers good process latitude and a large depth-of-focus, aspects that are esential for sidewall patterning. In addition, the development and exposure parameters are independent of substrate material, making the process equally applicable to InP, GaAs, and silicon. Although exposure times in our research apparatus can be

hours, it is well known that with production-type x-ray sources (synchrotron or laser plasmas) exposure times would be a few seconds.

II. DEVICE DESCRIPTION AND DESIGN

Figure 1 is a schematic of the ridge-waveguide sidewall-grating DFB laser. As shown, the grating is patterned on the sidewalls and both sides of the ridge. Feedback occurs due to the interaction of the lateral fields and the index modulation introduced by the grating. Since the mode profile falls off rapidly with distance, it is desirable to pattern the grating as far up along the sidewall as possible. Gratings are not patterned on top of the ridge to allow for a metal contact for current injection. Fabrication consists of materials growth, waveguide formation, and grating formation, with each step independent of the other two.

Figure 2 shows a schematic of a ridge-waveguide sidewall-grating DFB laser with a typical layer structure (InAlAs/InP), along with the important design parameters: the ridge width w, the ridge sidewall angle ϕ, the grating depth δ, and the distance from the lateral surface of the waveguide to the top graded index (GRIN) layer t_1. Computer simulations were carried out to calculate the coupling coefficient κ for a range of values of w, ϕ, δ, and t_1. The operating wavelength was taken to be 1.55 μm and the distance from the top of the ridge to the top GRIN layer was fixed at 1.5 μm. For a w of 3 μm, a ϕ of 60°, a δ of 200 nm, and a t_1 of 0.1 μm, the coupling coefficient κ was calculated to be 54.8 cm^{-1}. To reduce the effects of spatial-hole burning,[7] one should target a κL product of ~1.25, where L is the grating length. For $\kappa L=1.25$, the grating length is ~225 μm. For the parameters given above and the layer structure shown in Fig. 2, it was found that 33.5% of the coupling is due to the sidewall gratings, and the remaining 66.5% to the gratings on the flat surfaces.
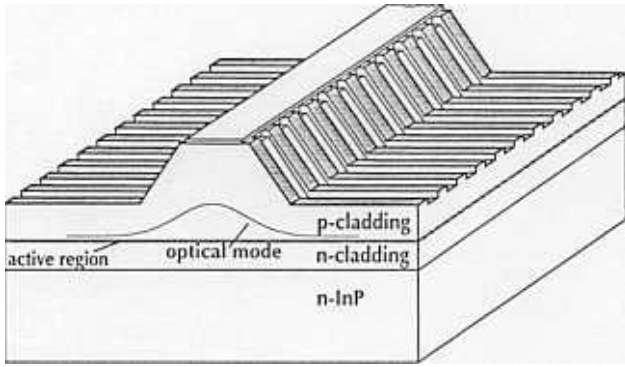
FIG. 1. Schematic of ridge-waveguide sidewall-grating DFB laser.

III. FABRICATION PROCESS

Our fabrication process consisted of the following steps. First, a contact metal is defined by lifting-off Ti/Pt/Au. This metal serves two purposes: as an electrode for current injection, and to prevent gratings from being patterned on top of the ridge. Next, a ridge waveguide is etched chemically into the substrate of choice. We used two materials systems: InAlAs lattice matched to InP and GaAs. After etching, 100 nm of SiO_x, which serves as a dry-etch mask for the RIE of the semiconductor, is sputtered. The substrate is then coated with poly(methylmethacrylate) (PMMA) resist (950 K molecular weight) and baked at 180 °C for 1 h. A first-order grating with a period of 230 nm is then patterned into the PMMA using XRL. We utilize an electron-bombardment source at the Cu_L line ($\lambda = 1.32$ nm).[8,9]

Present-day EBL systems suffer from field distortion, drift, and stitching errors,[10–12] which prevent one from having DFB gratings with long-range spatial-phase-coherence. Such coherence is necessary for single-mode operation and accurate control of the lasing wavelength, both of which are essential to high-performance optical communication systems [e.g., wavelength-division multiplexed (WDM) systems]. It was for these reasons that we used holographic lithography to make the x-ray mask.[12,13] How-
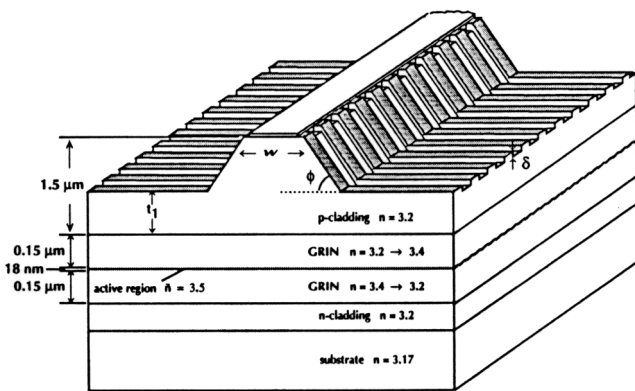

FIG. 2. Schematic of a ridge-waveguide sidewall-grating DFB laser showing a typical layer structure (InAlAs/InP) and the relevant design parameters.
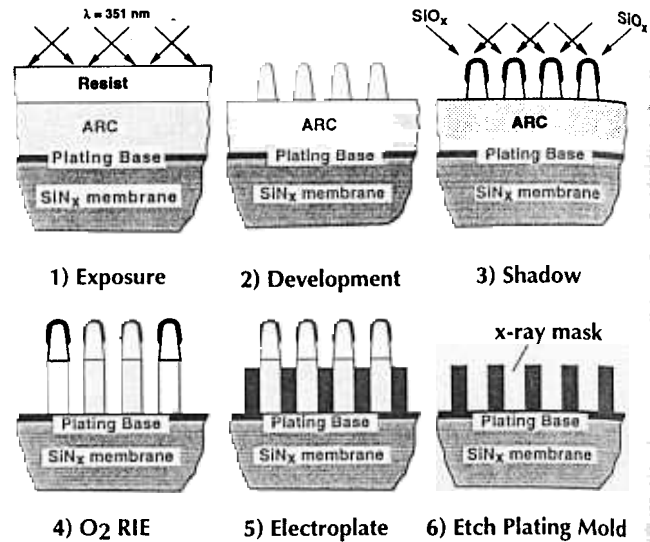
FIG. 3. Schematic of process for fabricating a grating x-ray mask by holographic lithography.

ever, a major advantage of using EBL is the ease with which a quarter-wave-shifted grating section can be included. It is well known that such a quarter-wave shift improves mode discrimination and decreases the laser linewidth.[14,15] To overcome the traditional difficulties of EBL, we are developing spatial-phase-locked EBL for fabricating x-ray masks for optoelectronic devices.[16]

The holographic lithography process is illustrated in Fig. 3. After cleaning the mask blank, a plating base (NiCr:Au; 5:20 nm) is evaporated. It is then immediately coated with 350 nm of antireflection coating (ARC)[17] and 195 nm of photoresist. A 230 nm-period grating is then holographically exposed ($\lambda = 351$ nm) and developed. The photoresist is then shadowed at $+35°$ and $-35°$ with 8.5 nm of e-beam evaporated SiO_x. The oxide serves as an etch mask during oxygen RIE through the ARC layer. A minimum of 20 nm of Au plating base is desirable to allow for some slight overetching. The x-ray mask is then gold-electroplated to a thickness of ~200 nm, which corresponds to 10 dB attenuation. The oxide is etched in dilute HF and the remaining resist and ARC stripped in an oxygen plasma.

After x-ray exposure the sample was immersion developed in a mixture of 1:2 methyl-isobutyi-ketone (MIBK): isopropyl alcohol (IPA) at 21 °C, followed by a rinse in ethyl alcohol and 1 min in an UV ozone cleaning system. A Ti/Al (30 nm/20 nm) etch mask was then lifted-off, followed by RIE in CHF_3 to etch through the oxide. RIE is then used to transfer the grating into the semiconductor. For etching InAlAs, a mixture of CH_4/H_2 gas is used, whereas for etching GaAs, $SiCl_4$.

IV. EXPERIMENTAL RESULTS AND DISCUSSION

For the ridge waveguides on InAlAs lattice matched to InP, an epitaxial layer grown by molecular-beam epitaxy was used, whereas for the ridge waveguides on GaAs, a bare substrate was used. Ridge waveguides 4–8 μm wide
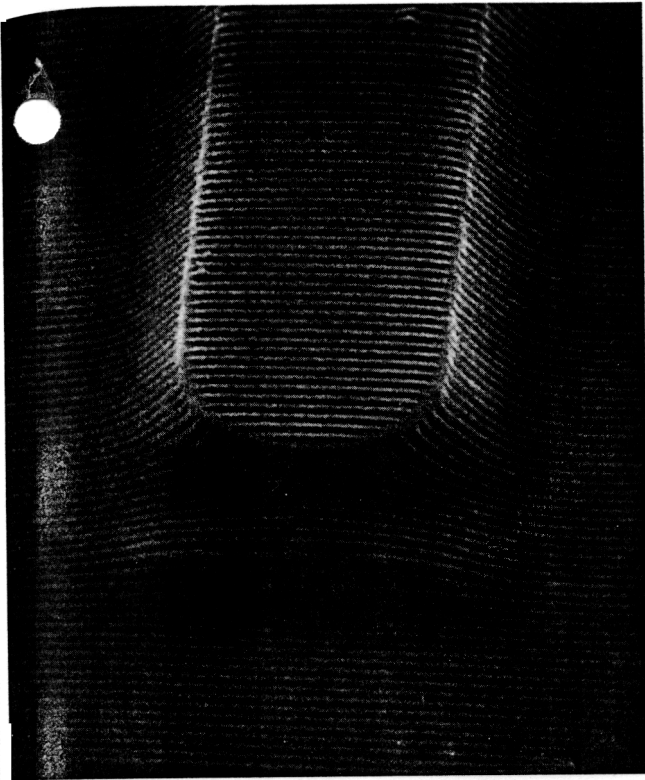
FIG. 4. SEM of PMMA grating (Λ=230 nm) lines defined using XRL on an InAlAs/InP ridge-waveguide. The ridge height is 1.0 μm, the side-wall angle is 60°, and the resist thickness 250 nm.
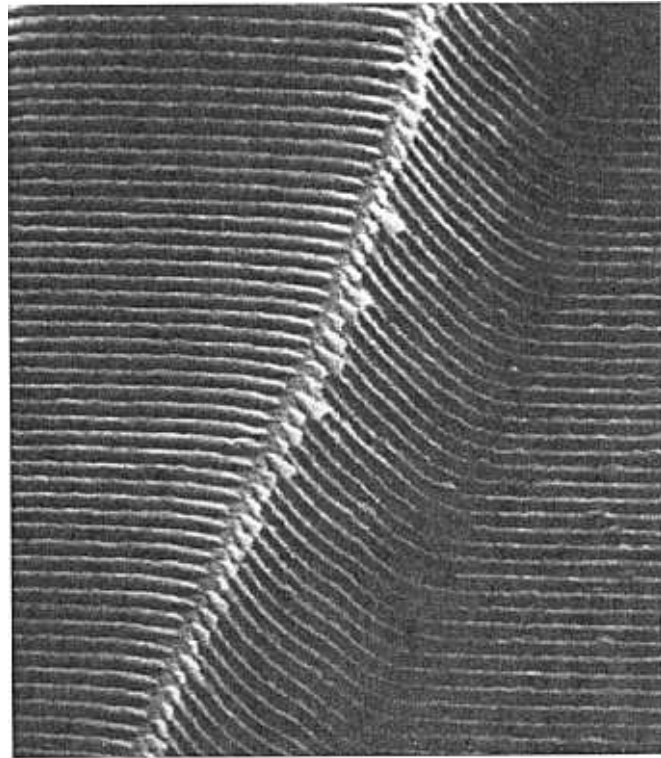

FIG. 5. SEM of Ti/Al (30/20 nm) grating lines (Λ=230 nm) on ridge waveguide on InAlAs/InP after lift-off.

were formed by wet-chemical etching with lithographically defined photoresist masks. A mixture of water, hydrogen peroxide, and phosphoric acid (1:10:1) was used for the wet-chemical etching. This particular combination was chosen so that the resulting ridges are crystallographically defined in the $\langle 1\bar{1}0 \rangle$ direction.[18] The ridge heights were varied from 1.0 μm for InAlAs/InP to 1.8 μm for GaAs since a typical ridge-stripe laser diode has a ridge height in this range.

Figure 4 shows a 230 nm-period grating in PMMA patterned over a 1.0 μm high InAlAs/InP ridge waveguide with a sidewall angle of 60°. The PMMA lines ride up the sidewalls and tends to be thinner on top than elsewhere due to planarization, as expected. The lift-off was straightforward, as shown in Fig. 5. It is worth noting that patterning PMMA lines onto the ridge sidewalls would be difficult with other lithographic techniques due to scattering from the ridge topography and the widely varying resist thickness.

To investigate if this process worked well with taller (i.e., more strongly confined) ridge waveguides, we pursued the result shown in Fig. 6: a 230 nm-period PMMA grating on a GaAs ridge waveguide with a height of 1.8 μm sidewall angle of 45°. It is clear from the figure that the resist near the top of the sidewall is thinner than the resist towards the bottom and over the bulk of the substrate. The high process latitude offered by XRL along with the high contrast offered by PMMA resist allows one
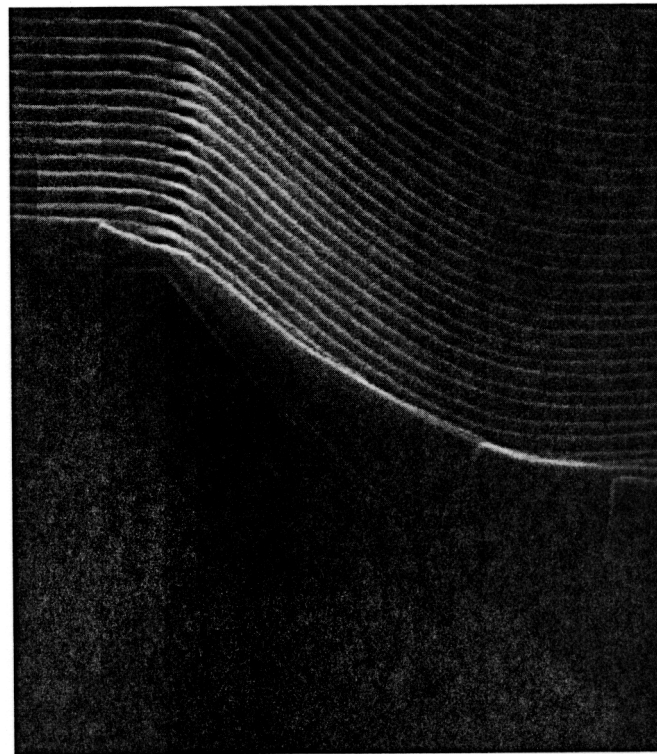

FIG. 6. SEM of PMMA grating (Λ=230 nm) lines defined using XRL on a GaAs ridge waveguide. The ridge height is 1.8 μm, the sidewall angle is 45°, and the resist thickness 500 nm.

to "over develop" the PMMA near the top of the sidewall without compromising the overall structure.

V. CONCLUSIONS

We have described progress in developing a novel ridge-waveguide DFB structure in which the grating is defined after both the materials growth and the guide formation. Such a structure avoids epitaxial regrowth and also permits independent control of the degree of lateral optical confinement. XRL was used to pattern 230 nm-period uniform gratings in PMMA onto ridge waveguides with heights up to 1.8 μm.

ACKNOWLEDGMENTS

[1] H. A. Haus and Y. Lai, IEEE J. Lightwave Technol. **LT-10**, 57 (1992).

[2] H. Temkin, R. A. Logan, N. A. Olsson, C. H. Henry, G. J. Dolan, R. F. Kazarinov, and L. F. Johnson, IEEE J. Lightwave Technol. **LT-4**, 520 (1986).

[3] C. J. Armistead, B. R. Butler, S. J. Clements, A. J. Collar, D. J. Moule, S. A. Wheeler, M. J. Fice, and H. Ahmed, Electron. Lett. **23**, 592 (1987).

[4] B. Borchert, B. Stegmuller, and R. Gessner, Electron. Lett. **29**, 210 (1993).

[5] L. M. Miller, J. T. Verdeyen, J. J. Coleman, R. P. Bryan, J. J. Alwan, K. J. Beernink, J. S. Hughes, and T. M. Cockerill, IEEE Photon. Technol. Lett. **3**, 6 (1991).

[6] M. Korn, T. Korfer, A. Forchel, and P. Roentgen, J. Vac. Sci. Technol. B **8**, 1404 (1990).

[7] H. Soda, H. Ishikawa, and H. Imai, Electron. Lett. **22**, 1047 (1986).

[8] A. Moel, M. L. Schattenburg, J. M. Carter, and H. I. Smith, J. Vac. Sci. Technol. B **8**, 1648 (1990).

[9] R. A. Ghanbari, W. Chu, E. E. Moon, M. Burkhardt, K. Yee, D. A. Antoniadis, M. L. Schattenburg, K. W. Rhee, R. Bass, M. C. Peckerar, and M. R. Melloch, J. Vac. Sci. Technol. B **10**, 3196 (1992).

[10] M. Korn, A. Forchel, M. Mohrle, R. Germann, K. Streubel, and F. Scholz, Microelectron. Eng. **6**, 571 (1987).

[11] T. Kjellberg and R. Schatz, IEEE J. Lightwave Technol. **LT-10**, 1256 (1992).

[12] E. H. Anderson, V. Boegli, M. L. Schattenburg, D. Kern, and H. I. Smith, J. Vac. Sci. Technol. B **9**, 3606 (1991).

[13] M. L. Schattenburg, C. R. Canizares, D. Dewey, K. A. Flanagan, M. A. Hamnett, A. M. Levine, K. S. K. Lum, R. Manikkalingam, T. H. Markert, and H. I. Smith, Opt. Eng. **30**, 1590 (1991).

[14] H. A. Haus and C. V. Shank, IEEE J. Quantum Electron. **QE-12**, 532 (1976).

[15] K. Kojima, K. Kyuma, and T. Nakayama, IEEE J. Lightwave Technol. **LT-3**, 1048 (1985).

[16] J. Ferrera, V. V. Wong, S. Rishton, V. Boegli, E. H. Anderson, D. P. Kern, and H. I. Smith, J. Vac. Sci. Technol B **11**, 2342 (1993).

[17] Experimental ARC-XL-MIT, Brewer Science, Inc., Rolla, MO 65401.

[18] Y. Mori and N. Watanaba, J. Electrochem. Soc. **125**, 1510 (1978).